Penetration of Thundercloud Electric Fields into the Ionosphere and Magnetosphere 1. Middle and Subauroral Latitudes

C. G. PARK AND M. DEJNAKARINTRA[1]

Radioscience Laboratory, Stanford University, Stanford, California 94305

The mapping of thundercloud electric fields at middle and subauroral latitudes is investigated analytically as a three-dimensional boundary value problem. The electrical conductivity is represented by several piecewise exponential functions of altitude, and the anisotropy of the medium is taken into account above 70-km altitude. The geomagnetic field lines are assumed to be straight and vertical below 150-km altitude. Electric field strength at great heights depends sensitively on conductivity and thundercloud models used in the calculations. Sample calculations using representative nighttime profiles show that 'giant' thunderclouds can produce transverse electric fields of tens of microvolts per meter in the equatorial plane of the midlatitude magnetosphere. In the daytime, corresponding electric fields are about an order of magnitude less. These results suggest that giant thunderclouds may be an important source of localized electric fields that can form field-aligned electron density irregularities in the ionosphere and the magnetosphere.

In the classical picture of atmospheric electricity, electric fields of tropospheric origin are confined within a spherical shell between the earth's surface and a conducting layer above ~60 km altitude. This conducting layer is below the ionosphere and is sometimes referred to as the potential equalizing layer or the electrosphere. The electrosphere, being a perfect conductor, forms an equipotential sphere around the earth and shields the space outside from electrical activity within.

Such a picture is substantially correct from the standpoint of atmospheric electricity. Electric fields found at ionospheric heights and above are typically $\sim 10^{-2}$ v/m or less, certainly negligible compared to fields of up to $\sim 10^{5}$ v/m near thunderclouds. From the point of view of ionospheric and magnetospheric physics, however, electric fields of much less than 10^{-2} v/m may have profound effects, and any possible source of fields as small as 10^{-5} v/m cannot be ignored.

Park and Helliwell [1971] discussed the role of localized electric fields in the formation of field-aligned electron density irregularities in the ionosphere and magnetosphere such as VLF and HF ducts. In this mechanism, irregularities are formed by mixing tubes of ionization with different content through $\mathbf{E} \times \mathbf{B}$ drift. The authors showed that electric fields of the order of 10^{-4} v/m in the magnetosphere are important for the formation of whistler ducts and suggested that giant thunderclouds may provide possible sources of such fields. This study was undertaken to investigate such a possibility. Our theoretical results indicate that electric fields from thunderclouds may indeed be important in the magnetosphere, although quantitative predictions are difficult because many parameters are poorly known at present. More experimental data on thunderclouds and atmospheric conductivity are needed for further progress in studies of electrostatic coupling between the troposphere and the ionosphere.

In this paper, discussion is limited to middle and subauroral latitudes where the magnetic field lines can be assumed to be vertical. Different formulations are required at low and equatorial latitudes and will be treated in a separate paper. Several authors have considered the mapping of electrostatic fields in various parts of the earth's surroundings, including *Holzer and Saxon* [1952], *Farley* [1959, 1960], *Spreiter and Briggs* [1961*a*, *b*], *Anderson and Freier* [1969], *Mozer and Serlin* [1969], *Mozer*

[1]On leave from Chulalongkorn University, Bangkok, Thailand.

[1970], *Atkinson et al.* [1971], *Illingworth* [1972], *Volland* [1972].

THEORY

We represent thunderclouds by electric charge centers of positive and negative polarity. The simplest model is a vertical dipole, but more complex arrangements of charge centers can also be used without difficulty. We seek analytical solutions for electric fields around a point charge from considerations of electric currents, conductivities, and appropriate boundary conditions. The total electric field resulting from a thundercloud can then be found by superposition of these solutions.

The electrical properties of the medium change greatly between thundercloud altitudes and the magnetosphere. Therefore we divide the space into several regions that require different treatment (Figure 1). At low altitudes where collision frequencies are large compared to gyrofrequencies the effects of the geomagnetic field are unimportant, and scalar conductivities can be used. At higher altitudes, say above 70 km, the anisotropy of the medium becomes important, and the conductivities must be represented by tensors. Above ~150 km, conductivities along the magnetic field become very large compared to transverse conductivities; thus the magnetic field lines can be considered equipotentials. Justifications will be given later for the choice of 70 and 150 km as demarcation levels. Since we are only concerned with middle and subauroral latitudes in this paper, geomagnetic field lines below 150 km are assumed to be straight and vertical. A dipole magnetic field is assumed above 150 km.

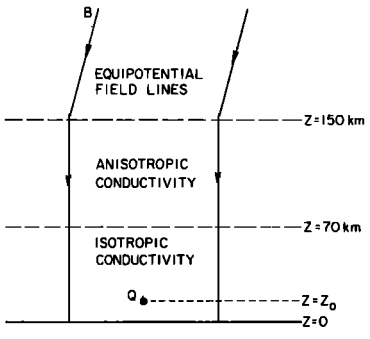

Fig. 1. A sketch of the simplified geomagnetic field and three different regions of its influence.

We will consider the region below 150 km in this section and the next. The mapping of electric fields between the 150-km level and the magnetosphere will then be treated.

Basic Equations

The equations to be solved are

$$\mathbf{J} = \boldsymbol{\sigma}\mathbf{E} \tag{1}$$

$$\mathbf{E} = -\nabla\Phi \tag{2}$$

$$\nabla \cdot \mathbf{J} = 0 \tag{3}$$

where $\boldsymbol{\sigma}$ is the conductivity tensor, and the other symbols have the usual meaning. We adopt a Cartesian coordinate system illustrated in Figure 2. The magnetic field **B** lies in the yz plane. The conductivity tensor is then written

$$\boldsymbol{\sigma} = \begin{bmatrix} \sigma_1 & \sigma_2 S & \sigma_2 C \\ -\sigma_2 S & \sigma_1 S^2 + \sigma_0 C^2 & (\sigma_1 - \sigma_0)CS \\ -\sigma_2 C & (\sigma_1 - \sigma_0)CS & \sigma_1 C^2 + \sigma_0 S^2 \end{bmatrix}$$

where

$$S = \sin I \qquad C = \cos I$$

σ_0, σ_1, and σ_2 are specific, Pedersen, and Hall conductivities, respectively, and I is the magnetic dip angle or the angle between **B** and the y axis.

If we assume a horizontally stratified medium (i.e., $\partial\sigma/\partial x = \partial\sigma/\partial y = 0$), equations 1, 2, and 3 can be combined to yield

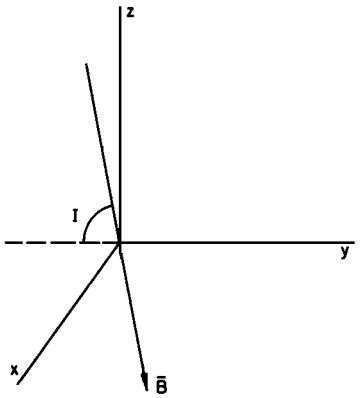

Fig. 2. A sketch of the Cartesian coordinate system used in deriving (4). The magnetic field vector **B** lies in the yz plane.

$$\frac{\partial^2\Phi}{\partial x^2} + \left(S^2 + \frac{\sigma_0}{\sigma_1} C^2\right)\frac{\partial^2\Phi}{\partial y^2} + \left(\frac{\sigma_0}{\sigma_1} S^2 + C^2\right)\frac{\partial^2\Phi}{\partial z^2} + 2\left(1 - \frac{\sigma_0}{\sigma_1}\right)SC\,\frac{\partial^2\Phi}{\partial y\,\partial z} - \frac{C}{\sigma_1}\frac{\partial\sigma_2}{\partial z}\frac{\partial\Phi}{\partial x} + \frac{SC}{\sigma_1}\frac{\partial(\sigma_1 - \sigma_0)}{\partial z}\frac{\partial\Phi}{\partial y} + \frac{1}{\sigma_1}\left(S^2\frac{\partial\sigma_0}{\partial z} + C^2\frac{\partial\sigma_1}{\partial z}\right)\frac{\partial\Phi}{\partial z} = 0 \qquad (4)$$

This differential equation cannot be solved analytically for arbitrary values of S and C. However, at middle and high geomagnetic latitudes, where $I \cong 90°$, (4) can be greatly simplified if we set $S = 1$ and $C = 0$:

$$\frac{\partial^2\Phi}{\partial x^2} + \frac{\partial^2\Phi}{\partial y^2} + \frac{1}{\sigma_1}\frac{\partial}{\partial z}\left(\sigma_0\frac{\partial\Phi}{\partial z}\right) = 0 \qquad (5)$$

This equation can now be solved analytically by the method of separation of variables.

Solutions

We first transform (5) to cylindrical coordinates and assume axial asymmetry:

$$\frac{\partial^2\Phi}{\partial r^2} + \frac{1}{r}\frac{\partial\Phi}{\partial r} + \frac{1}{\sigma_1}\frac{\partial}{\partial z}\left(\sigma_0\frac{\partial\Phi}{\partial z}\right) = 0 \qquad (6)$$

Following the standard procedure, we let

$$\Phi = R(r)Z(z) \qquad (7)$$

and, by substituting this in (6), we obtain

$$\frac{d^2R}{dr^2} + \frac{1}{r}\frac{dR}{dr} + k^2R = 0 \qquad (8)$$

$$\frac{1}{\sigma_1}\frac{d}{dz}\left(\sigma_0\frac{dZ}{dz}\right) - k^2Z = 0 \qquad (9)$$

where k is a separation constant.

The solution to (8) can be written in terms of Bessel functions:

$$R(r) = AJ_0(kr) + BN_0(kr)$$

J_0 and N_0 are the zero-order Bessel functions of the first kind and the second kind, respectively. The boundary condition that Φ remains finite as $r \to 0$ requires that $B = 0$. Hence

$$R(r) = AJ_0(kr) \qquad (10)$$

To solve (9), the z dependence of σ_0 and σ_1 must be specified. We assume they both vary as $e^{z/\alpha}$. This does not limit the applicability of the solutions obtained, because any reasonable conductivity profile can be closely approximated by a series of simple exponential functions (see next section). The solutions for Φ will be obtained separately for isotropic and anisotropic regions. We will consider the simpler case of isotropic conductivity first.

Isotropic conductivity. If we let $\sigma_0 = \sigma_1 = \sigma = ae^{z/\alpha}$, equation 9 becomes

$$\frac{d^2Z}{dz^2} + \frac{1}{\alpha}\frac{dZ}{dz} - k^2Z = 0 \qquad (11)$$

The solution to this equation is

$$Z(z) = Ae^{m_1 z} + Be^{m_2 z} \qquad (12)$$

where

$$m_1 = -\frac{1}{2\alpha} - \left(\frac{1}{4\alpha^2} + k^2\right)^{1/2}$$

$$m_2 = -\frac{1}{2\alpha} + \left(\frac{1}{4\alpha^2} + k^2\right)^{1/2}$$

and A and B are arbitrary constants.

Anisotropic conductivity. We assume that σ_0 and σ_1 vary exponentially with altitude above a reference level $z = h_0$ and write

$$\sigma_0 = \sigma_{00}\exp\left[(z - h_0)/\alpha_0\right]$$

$$\sigma_1 = \sigma_{10}\exp\left[(z - h_0)/\alpha_1\right]$$

Substituting these in (9), we obtain

$$\frac{d^2Z}{dz^2} + \frac{1}{\alpha_0}\frac{dZ}{dz} - \frac{\sigma_{10}}{\sigma_{00}}\cdot\left\{\exp\left[-(z - h_0)\left(\frac{1}{\alpha_0} - \frac{1}{\alpha_1}\right)\right]\right\}k^2Z = 0 \qquad (13)$$

This equation can be rewritten in the form of a transformed Bessel equation

$$u^2\frac{d^2Z(u)}{du^2} - \gamma u\frac{dZ(u)}{du} - u^2k^2Z(u) = 0 \qquad (14)$$

by introducing a new variable

$$u = C(\sigma_{10}/\sigma_{00})^{1/2}\exp\left[-(z - h_0)/C\right]$$

and new constants

$$\gamma = \frac{\alpha_1 + \alpha_0}{\alpha_1 - \alpha_0}$$

$$\frac{1}{C} = \frac{1}{2}\left(\frac{1}{\alpha_0} - \frac{1}{\alpha_1}\right)$$

The solution to (14) can be written in terms of Bessel functions [e.g., *Spiegel*, 1968, or *Farrell and Ross*, 1971]:

$$(Z)u = (ku)^{\nu}[AI_{\nu}(ku) + KB_{\nu}(ku)] \qquad (15)$$

where

$$\nu = \alpha_1/(\alpha_1 - \alpha_0)$$

I_ν and K_ν are modified Bessel functions of the first and the second kind, respectively, and of order ν.

Since we now have solutions for Φ, the horizontal electric field can be obtained by differentiation:

$$E_r = -\partial\Phi/\partial r$$

From (7), (10), (12), and (15), we obtain

$$E_r = \int_0^\infty J_1(kr)\{A_1(k) \exp [m_1(k)z] + B_1(k) \exp [m_2(k)z]\}k\, dk \qquad (16)$$

for the isotropic region and

$$E_r = \int_0^\infty J_1(kr)[A_2(k)I_\nu(ku) + B_2(k)K_\nu(ku)]u^\nu k^{\nu+1}\, dk \qquad (17)$$

for the anisotropic region.

The actual conductivities are not simple exponential functions of altitude in the entire region of interest (see Figure 3). However, they can be divided into a number of sections within which the σ's are approximated by simple exponential functions with constant scale heights. Equation 16 or 17 would apply within each section. If there are N such sections, we obtain N equations with $2N$ arbitrary constants, which must be evaluated by as many boundary conditions.

Boundary Conditions

Equations 16 and 17 are subject to the following boundary conditions:

$\Phi = 0$ at $z = 0$.

$E_z = 0$ at $z = 150$ km.

E is continuous across the boundary at $z = z_0$ except for a jump in E_z at $r = 0$ by an amount Q/ϵ_0 [e.g., *Panofsky and Phillips*, 1962].

E is continuous at intermediate section boundaries.

The second boundary condition above is equivalent to the assumption of equipotential geomagnetic field lines, and the results of the next section will show that this assumption is well justified at $z = 150$ km. If the third boundary condition is used to relate the magnitude of **E** to Q, (16) and (17) become

$$E_r = \frac{Q}{2\pi\epsilon_0}\int_0^\infty J_1(kr)\{a_1(k) \exp [m_1(k)z] + b_1(k) \exp [m_2(k)z]\}k\, dk \qquad (18)$$

$$E_r = \frac{Q}{2\pi\epsilon_0}\int_0^\infty J_1(kr)[a_2(k)I_\nu(ku) + b_2(k)K_\nu(ku)]u^\nu k^{\nu+1}\, dk \qquad (19)$$

E_r is proportional to Q everywhere. An examination of (18) and (19) reveals an important result: E_r depends on the height variations of the conductivities but not on their absolute values. The integrals in (18) and (19) can be evaluated numerically once the coefficients $a(k)$ and $b(k)$ are determined from the boundary conditions.

CALCULATIONS AND RESULTS

In this section, we present the results of electric field calculations and discuss their dependence on electrical conductivity and thundercloud models.

Conductivity profile

The electrical conductivity of the atmosphere and the lower ionosphere is not yet well known, but Figure 3 shows several representative

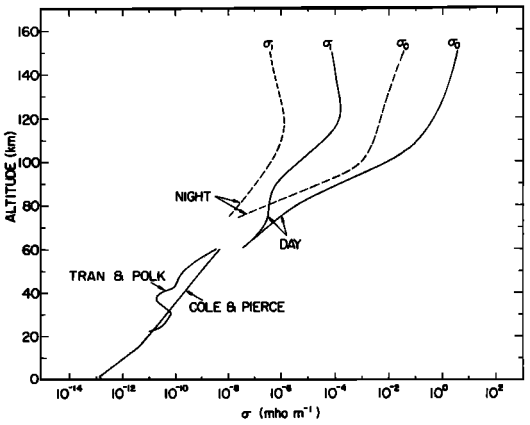

Fig. 3. A composite of representative conductivity profiles. See text for sources of data.

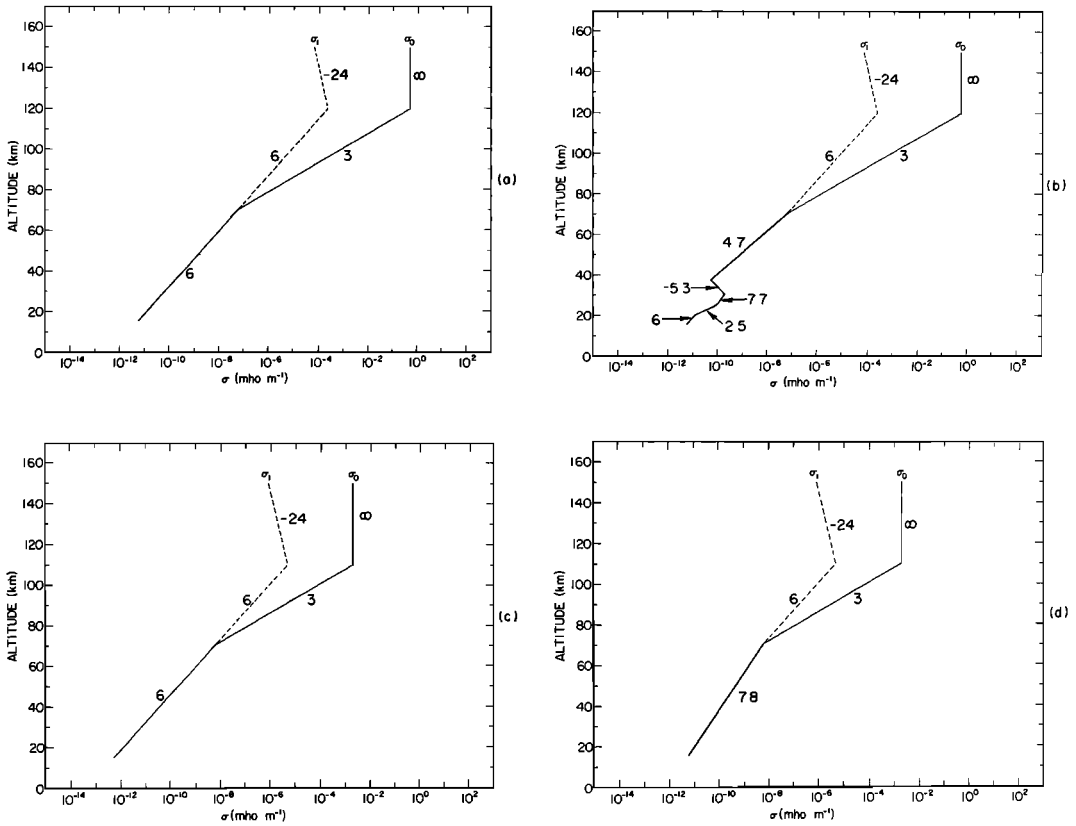

Fig. 4. (*a*) Conductivity model A approximates the daytime profile above 70 km, the Cole and Pierce profile below 70 km. The numbers next to the curves are scale heights in kilometers. (*b*) Conductivity model B approximates the daytime profile above 70 km, the Tran and Polk profile below 70 km. (*c*) Conductivity model C approximates the nighttime profile above 70 km; below 70 km, it has the same scale height as the Cole and Pierce profile. *(d)* Conductivity model D approximates the nighttime profile above 70 km and has the same value as the Cole and Pierce profile at 20 km.

conductivity profiles based on information currently available. Below 60 km, *Cole and Pierce*'s [1965] theoretical model is shown together with a profile calculated by *Tran and Polk* [1972]. The latter is based on *Bragin*'s [1967] rocket measurements of ion concentrations. Between 60 and 120 km, electron concentration data recently compiled by *Maeda* [1971] and the U.S. Standard Atmosphere (1966) are used to calculate σ_0 and σ_1 according to the formulas given by *Hanson* [1961]. The daytime profile is based on the mean electron concentration profile for spring and fall near sunspot minimum (Maeda's model SF-A); the nighttime profile represents conditions near local midnight averaged over all seasons and solar activity levels (Maeda's model N2). Figure 4(*a–d*) shows conductivity models used in the calculations below for daytime and nighttime conditions. In all models the atmosphere becomes anisotropic above 70 km. These profiles are intended to represent conditions at middle and subauroral latitudes. Conductivities are very different at auroral and higher latitudes, but they will not be considered here, since thunderstorms are not likely to occur at those latitudes.

Electric Fields due to Monopoles

We now examine the behavior of the horizontal electric field E_r calculated for a monopole of charge Q located at an altitude of z_0. Since E_r is proportional to Q, all results will be

shown normalized to $Q = 1$ coulomb. For sample calculations in this subsection, z_0 was assumed to be 15 km. The next subsection will show how the results depend on z_0.

Figure 5 shows how E_r varies with r at several altitudes. Conductivity model C was used. E_r first rises to a maximum and then falls off exponentially at large values of r. As z increases, the E_r curve becomes broader and the peak moves outward until it reaches $r \cong 40$ km at $z = 100$ km. E decreases rapidly with altitude at first but levels off near $z = 90$ km (also see Figure 7). These general features of E_r are the same for all conductivity models.

In Figure 6, E_r is plotted against z at several values of r for conductivity models A and B. For model A, E_r decreases nearly exponentially with altitude. The irregular profile in model B causes E_r to be nearly constant with altitude in the region of irregularity. At large z, E_r for the two models becomes almost identical (also see Figure 7).

Figure 7 shows the maximum E_r as a function of altitude for the four conductivity models. All four curves show similar behavior, but the magnitude of $E_{r,\max}$ at large z depends sensitively on the model. For the same cloud parameters, much larger electric fields are predicted at night than in the daytime. At the 150-km level, $E_{r,\max}$ occurs at $r_{\max} = 35$–40 km for all four models. The shape of the E_r distribution

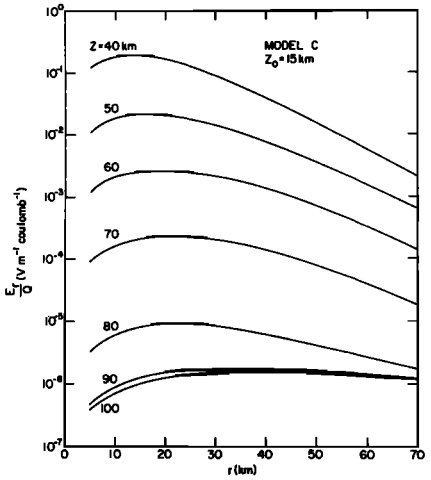

Fig. 5. Normalized horizontal electric field due to a monopole plotted against horizontal distance from the monopole.

at large heights does not depend sensitively on the conductivity profile.

Below ~90 km, the rate of decrease of $E_{r,\max}$ with z is related to conductivity scale heights. Thus the changes in slopes at 70 km reflect changes in scale heights of σ_0. Above ~90 km, electric fields become nearly constant with altitude. This agrees with the results of *Spreiter and Briggs* [1961*a*], who found that electric fields with horizontal dimensions of more than a few kilometers at the 100 km level can reach the F region with little attenuation. The reason for this behavior is that at these altitudes σ_0 is much greater than σ_1, and magnetic field lines become nearly equipotentials. In Figure 7 magnetic field lines were forced to become equipotentials at $z = 150$ km, but nearly identical results are obtained if this condition is imposed at infinity rather than at 150 km. This justifies the upper boundary condition at 150 km.

Below 70 km, where conductivity is isotropic, the important parameter is the number of conductivity scale heights between the charge and the altitude of interest. For example, models A and B represent different height variations of conductivity below 70 km, but they both involve the same number of scale heights between 15 and 70 km. The two models give nearly identical $E_{r,\max}$. For models C and D there are 9.2 and 7.1 scale heights, respectively, between 15 and 70 km. The ratio of $E_{r,\max}$ at $z = 70$ km between the two models is ~7, close to the value of $e^{2.1} = 8$.

Dependence on z_0

Figure 8(*a*) illustrates how $E_{r,\max}$ depends on z_0. $E_{r,\max}$ at $z = 150$ km was calculated for model C and for different values of z_0. The results are normalized to the value of $Q = 1$ coulomb at $z_0 = 5$ km. The value of r where $E_{r,\max}$ occurs is shown in Figure 8(*b*). For $z_0 \gtrsim 7$ km, $E_{r,\max}$ increases exponentially with z_0. The e folding height of $E_{r,\max}$ is the same as the conductivity scale height. Thus, if z_0 is changed by an amount Δz_0, $E_{r,\max}$ changes by a factor e^N, where N is the number of conductivity scale heights in Δz_0. This is also true for other conductivity models. The $E_{r,\max}$ curve becomes much steeper as z_0 decreases below ~7 km owing to induced charges on the ground. The effect of the image charge is negligible when z_0 is large but becomes noticeable

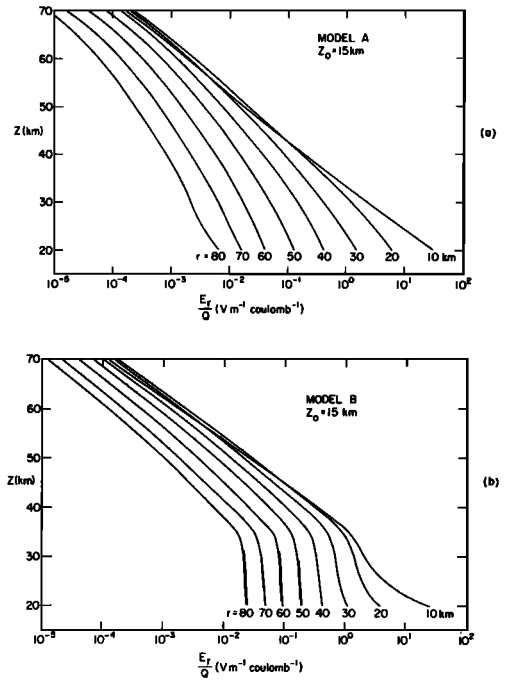

Fig. 6. Normalized horizontal electric field due to a monopole plotted against altitude for conductivity models A and B.

when z_0 is comparable to the conductivity scale height α_0.

The shape of electric field distribution at large heights does not depend sensitively on z_0. At 150 km, the peak of the E_r distribution moves inward by only ~5 km when z_0 is changed from 5 to 25 km. The shape of the E_r distribution is also insensitive to conductivity models, as was pointed out earlier.

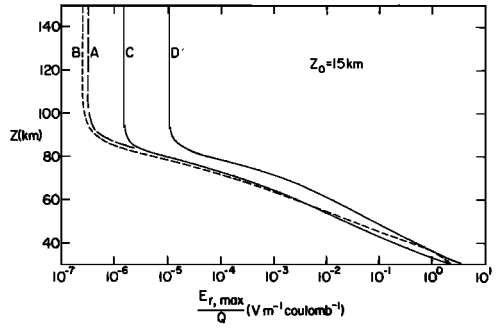

Fig. 7. Normalized maximum horizontal electric field due to a monopole plotted as a function of altitude for conductivity models A, B, C, and D.

Thundercloud model

The simplest thundercloud model is a vertical dipole with charge $+Q$ at the top and $-Q$ below. Some cloud models include small positive charges near the bottom of the cloud in addition to a dipole [e.g., *Uman*, 1969]. Electric fields due to each charge center can be calculated separately as above and then added to obtain the total field. Because E_r decreases rapidly with decreasing z_0, charges at lower altitudes can be ignored if they are located more than one conductivity scale height below the uppermost charge center (see Figure 8).

The altitude of charge centers varies widely, depending upon the size of the thundercloud. In 'giant' thunderclouds which extend from a few to 20 or more km in altitude [*Uman*, 1969; *Workman*, 1965; *Vonnegut and Moore*, 1958], the positive charge center may be at ~15 km and the negative center at ~5 km. In 'typical' thunderclouds, the upper charge center may be at ~10 km.

Estimates of the magnitude of Q vary widely, but for giant thunderclouds the uppermost positive charge may be ~50 coulombs or more

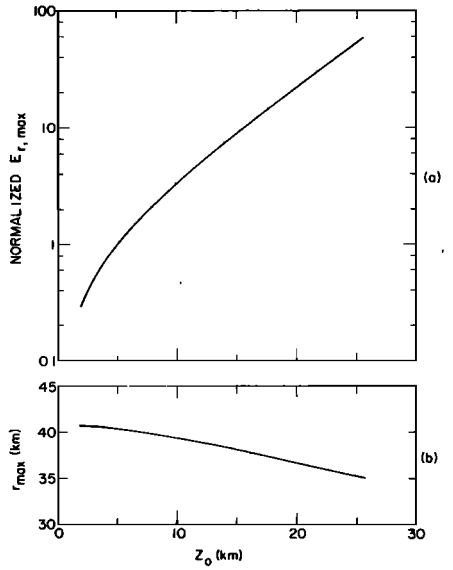

Fig. 8. (*a*) Maximum horizontal electric field for model C at the 150-km level as a function of the monopole altitude. The field strength is normalized to the value corresponding to 1 coulomb charge at 5-km altitude. (*b*) A plot of horizontal distance from the monopole where $E_{r,max}$ occurs at the 150 km level.

[*Malan*, 1963; *Kasemir*, 1965]. If we assume +50 coulombs at 15 km and ignore the effects of charge centers at lower altitudes, we obtain $E_{r,\max} = 20$, 15, 90, and 650 μv/m at $z = 150$ km for conductivity models A, B, C, and D, respectively. Lowering the uppermost charge from 15- to 10-km altitude would reduce the corresponding electric fields by a factor of ~3. If there are several thunderclouds in a storm area, their effects are additive. We can see from Figure 5 that thunderclouds within ~100-km radius may contribute significantly to the total $E_{r,\max}$.

The thundercloud is represented here by electrostatic charges. These charges are assumed to be maintained by the thundercloud electrification process, which also supplies conduction currents flowing within and around the cloud. When lightning discharges occur, however, these charges suffer rapid fluctuations. The problem of time-varying sources will be treated in a separate paper.

ELECTROSTATIC FIELD MAPPING ABOVE 150 KILOMETERS

Above 150 km geomagnetic field lines are considered equipotentials. The mapping of electric fields in this case depends simply on the magnetic field line geometry. We will first derive general formulas for mapping factors between any two arbitrary points on a field line.

In a dipole approximation, the magnetic field strength B is given by

$$B = B_0\left(\frac{R_0}{r}\right)^3(1 + 3\sin^2\phi)^{1/2} \qquad (20)$$

where r and ϕ are geocentric distance and latitude, respectively. R_0 is the mean radius of the earth, and B_0 is the value of B at $r = R_0$ and $\phi = 0$. The equation for a dipole field line is

$$r/(\cos^2\phi) = \text{constant} \qquad (21)$$

Consider a tube of force in the magnetosphere as sketched in Figure 9. The mapping factor for the east-west component of electric field is

$$\frac{E_{w1}}{E_{w2}} = \frac{W_2}{W_1} = \frac{r_2\cos\phi_2}{r_1\cos\phi_1} \qquad (22)$$

Using (21), we obtain

$$\frac{E_{w1}}{E_{w2}} = \left(\frac{\cos\phi_2}{\cos\phi_1}\right)^3 \qquad (23)$$

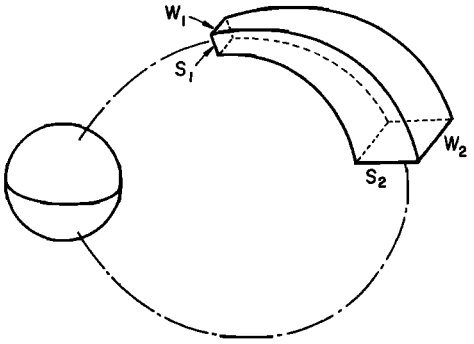

Fig. 9. A sketch of a flux tube in the magnetosphere.

Since the magnetic flux is constant in the tube, we can write

$$\frac{W_2S_2}{W_1S_1} = \left(\frac{r_2}{r_1}\right)^3\left(\frac{1 + 3\sin^2\phi_1}{1 + 3\sin^2\phi_2}\right)^{1/2} \qquad (24)$$

From (21), (22), and (24),

$$\frac{E_{s1}}{E_{s2}} = \left(\frac{\cos\phi_2}{\cos\phi_1}\right)^3\left(\frac{1 + 3\sin^2\phi_1}{1 + 3\sin^2\phi_2}\right)^{1/2} \qquad (25)$$

If we consider mapping from an arbitrary latitude ϕ to the equatorial plane ($\phi = 0$), equations 23 and 25 become

$$\frac{E_{weq}}{E_w} = \cos^3\phi \qquad (26)$$

$$\frac{E_{seq}}{E_s} = \frac{\cos^3\phi}{(1 + 3\sin^2\phi)^{1/2}} \qquad (27)$$

where the subscript eq refers to the equatorial plane. These quantities are plotted in Figure 10 as a function of ϕ.

The mapping factors are different for east-west and north-south electric fields. Thus the cylindrical symmetry of the electric fields at 150 km is destroyed when they are mapped to the equatorial plane. At $L = 4$, ϕ at 150 km altitude is close to 60°, and the mapping factors for east-west and north-south electric fields are 0.12 and 0.08, respectively. The results of the preceding section showed that the locus of $E_{r,\max}$ at 150 km is a circle with ~70-km diameter. In the equatorial plane at $L = 4$ this transforms into an ellipse with an 840-km major axis in the radial direction and a 560-km minor axis in the east-west direction.

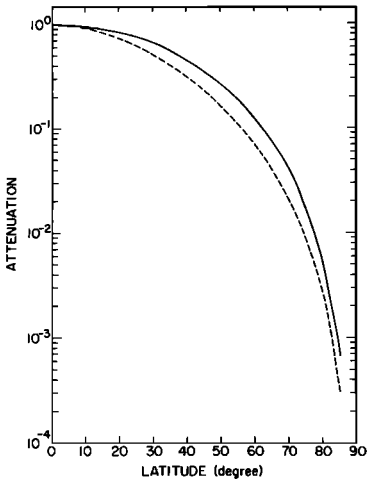

Fig. 10. Attenuation factors for east-west (*solid line*) and north-south (*dotted line*) electric fields when mapping from an arbitrary geomagnetic latitude to the equatorial plane. A dipole geomagnetic field is assumed.

DISCUSSION

The results presented here indicate that thunderclouds may provide important sources of localized electric fields in the ionosphere and the magnetosphere. These electric fields can produce field-aligned irregularities by mixing tubes with different plasma content through $\mathbf{E} \times \mathbf{B}$ drift. The resulting irregular structures depend on both the initial tube content and electric field distributions. *Park and Helliwell* [1971] showed that an extremely complex structure can evolve from a very simple initial condition and a very simple electric field distribution.

To form a whistler duct by this mechanism, the electric field must have a suitable size, as well as sufficient field strength. We will consider the question of scale size first. The transverse dimensions of whistler ducts are believed to be tens of kilometers at ionospheric heights [*Angerami*, 1970]. The scale size of electric fields found above is ~70 km at 150-km altitude and is therefore suitable for forming whistler ducts. It was also found that the scale size does not depend sensitively on the conductivity or the cloud model used in the calculations. The size of an electric field puts an upper limit on the size of irregularities it can produce, but there is no lower limit. Thus thundercloud electric fields may also be important for smaller scale irregularities such as HF ducts with dimensions of the order of several kilometers [*Muldrew*, 1967].

The question of electric field strength is more complex, both in terms of what is needed to form whistler ducts and what is available from thunderclouds. Thundercloud electric fields of 15–650 μv/m were calculated at 150-km altitude. Unlike the scale size, the magnitude of electric fields depends sensitively on conductivity and cloud models used in the calculations. In view of the uncertainties in these parameters, we can reasonably expect an order of magnitude uncertainty in the electric field values quoted above. The field strength needed to form a duct depends on how long the field is applied, as well as on the initial electron distribution. *Park and Helliwell* [1971] showed that, if a uniform equatorial electron concentration is assumed as an initial condition, an electric field of 50 μv/m in the equatorial plane at $L = 4$ can form a duct in ~1 hour. This corresponds to ~500 μv/m at the 150-km level (see Figure 10). When we compare this with the thundercloud electric fields quoted above, it appears that thunderclouds may provide adequate electric fields to form whistler ducts. A more definitive test will be possible when more is known about the atmospheric conductivities and the electrical structure of thunderclouds.

When mapping tropospheric electric fields to ionospheric heights, it is important to include the effects of the geomagnetic field above ~70 km altitude. As a test, the calculations were repeated with identical parameters except σ_1 was made equal to σ_0 at all heights. At the 150-km level $E_{r,\max}$ thus calculated is more than 3 orders of magnitude smaller than in the case of anisotropic conductivity. (If conductivity is assumed to be isotropic everywhere, it is appropriate to let the potential Φ be constant at $z = \infty$ rather than at $z = 150$ km. This change in the upper boundary condition changes $E_{r,\max}$ at 150 km by only a factor of ~2.) It is also found that $E_{r,\max}$ occurs at $r_{\max} \cong 60$ km, larger than ~35 km for the anisotropic case. This can be understood in terms of a tendency for the geomagnetic field to bend electric flux lines toward the vertical.

As was pointed out earlier, electrostatic coupling between the troposphere and the iono-

sphere depends critically on height variations of electrical conductivity. Unfortunately it is not possible at present to make quantitative predictions of the coupled effects, because the conductivities are still poorly known. This is particularly true in the 30- to 80-km range, where rockets remain the only means of exploration. More measurements of conductivities are essential for further progress in this area of research. The electrical structure of thunderclouds needs to be better understood [e.g., *Kasemir*, 1965]. The cloud parameters deduced from ground measurements are most accurate with respect to the conditions in the lower portions of the cloud. On the other hand, the conditions near the cloud tops are more important for electric fields at great heights. More measurements of electric fields and conductivities above the cloud tops are needed to construct more accurate cloud models.

CONCLUSIONS

The results of this study suggest that thundercloud electric fields may play an important role in the formation of field-aligned electron density irregularities in the ionosphere and the magnetosphere. The scale size of horizontal electric fields at ionospheric heights is suitable for forming VLF and HF ducts. The field strength may also be adequate, but this question remains uncertain because the results depend sensitively on electrical conductivity and thundercloud models, which are not well known at present. More experimental data on atmospheric conductivity and thundercloud structure are essential for better understanding of electrostatic coupling between the troposphere, ionosphere, and magnetosphere.

Acknowledgments. We are grateful to Professor R. A. Helliwell for his continued support and encouragement throughout this research. We also thank Drs. E. T. Pierce and H. Dolezalek for helpful discussion.

This work was supported by the National Science Foundation, Atmospheric Sciences Section, under grant GA-28042. Computer facilities were sponsored in part by the Office of Computer Sciences of the National Science Foundation under grant GP-948.

* * *

The Editor thanks F. S. Mozer, B. Vonnegut, and another referee for their assistance in evaluating this paper.

REFERENCES

Anderson, F. J., and G. D. Freier, Interactions of the thunderstorm with a conducting atmosphere, *J. Geophys. Res., 74,* 5390, 1969.

Angerami, J. J., Whistler duct properties deduced from VLF observations made with the Ogo 3 satellite near the magnetic equator, *J. Geophys. Res., 75,* 6115, 1970.

Atkinson, W., S. Lundquist, and U. Fahleson, The electric field existing at stratospheric elevations as determined by tropospheric and ionospheric boundary conditions, *Pure Appl. Geophys., 84,* 46, 1971.

Bragin, I. A., Direct measurements of ion and electron concentration in the stratosphere and the mesosphere, *Space Res., 7,* 391, 1967.

Cole, R. K., and E. T. Pierce, Electrification in the earth's atmosphere for altitudes between 0 and 100 km, *J. Geophys. Res., 70,* 2735, 1965.

Farley, D. T., Jr., A theory of electrostatic fields in a horizontally stratified ionosphere subject to constant, vertical magnetic field, *J. Geophys. Res., 64,* 1225, 1959.

Farley, D. T., Jr., A theory of electrostatic fields in the ionosphere at nonpolar geomagnetic latitudes, *J. Geophys. Res., 65,* 869, 1960.

Farrell, O. J., and B. Ross, *Solved Problems in Analysis as Applied to Gamma, Beta, Legendre and Bessell Functions,* p. 313, Dover, New York, 1971.

Hanson, W. B., Structure of the ionosphere, *Satellite Environment Handbook,* edited by F. S. Johnson, p. 27, Stanford University Press, Stanford, Calif., 1961.

Holzer, R. E., and D. S. Saxon, Distribution of electrical conduction currents in the vicinity of thunderstorms, *J. Geophys. Res., 57,* 207, 1952.

Illingworth, A. J., Electric field recovery after lightning as the response of the conducting atmosphere to a field charge, *Quart. J. Roy. Meteorol. Soc., 98,* 604, 1972.

Kasemir, H. W., The thundercloud, in *Problems of Atmospheric and Space Electricity,* edited by S. C. Coroniti, p. 215, Elsevier, New York, 1965.

Maeda, K., Study of electron density profile in the lower ionosphere, *J. Geomag. Geoelec., 23,* 133, 1971.

Malan, D. J., *Physics of Lightning,* p. 56, The English University Press Ltd., 1963.

Mozer, F. S., Electric field mapping in the ionosphere at the equatorial plane, *Planet. Space Sci., 18,* 259, 1970.

Mozer, F. S., and R. Serlin, Magnetospheric electric field measurements with balloons, *J. Geophys. Res., 74,* 4739, 1969.

Muldrew, D. B., Medium frequency conjugate echoes observed on topside-sounder data, *Can. J. Phys., 45,* 3935, 1967.

Panofsky, W. K. H., and M. Phillips, *Classical Electricity and Magnetism,* 2nd ed., p. 91, Addison-Wesley, Reading, Mass., 1962.

Park, C. G., and R. A. Helliwell, The formation by electric fields of field-aligned irregularities in the magnetosphere, *Radio Sci., 6,* 299, 1971.

Spiegel, M. R., *Mathematical Handbook of Formulas and Tables,* p. 106 and p. 136, Schaum's Outline Series, McGraw-Hill, New York, 1968.

Spreiter, J. R., and B. R. Briggs, Theory of electrostatic fields in the ionosphere at polar and middle geomagnetic latitudes, *J. Geophys. Res., 66,* 1731, 1961*a*.

Spreiter, J. R., and B. R. Briggs, Theory of electrostatic fields in the ionosphere at equatorial latitudes, *J. Geophys. Res., 66,* 2345, 1961*b*.

Trân, A., and C. Polk, Lowest (40 km to 70 km) ionospheric conductivity profiles and Schumann (ELF) resonances, Report to Air Force Cambridge Research Laboratories on Contract F19628-70-C-0090, Univ. of Rhode Island, Dept. of Electrical Engineering, August 1972.

Uman, M. A., *Lightning,* p. 2, McGraw-Hill, New York, 1969.

Volland, H., Mapping of the electric field of the *Sq* current into the lower atmosphere, *J. Geophys. Res., 77,* 1961, 1972.

Vonnegut, B., and C. B. Moore, Giant electrical storms, *Recent Advances in Atmospheric Electricity,* edited by L. G. Smith, p. 399, Pergamon, London, 1958.

Workman, E. J., Thunderstorm electricity, in *Problems of Atmospheric and Space Electricity,* edited by S. C. Coroniti, p. 296, Elsevier, New York, 1965.

(Received November 30, 1972;
accepted April 24, 1973.)